

# NEURAL CLASSIFIER OF DEEP BRAIN STIMULATION EVOKED EMOTION

**Anonymous authors**

Paper under double-blind review

## ABSTRACT

Precise deep brain stimulation (DBS) of Subcallosal Cingulate White Matter (SC-Cwm) alleviates symptoms of treatment resistant depression (TRD). Objective signatures from neural recordings are needed to optimize implantation and programming of antidepressant brain stimulation, and recent advances in machine learning help identify these in noisy patient recordings. In this study, we present a machine learning classifier build from previously reported dense-array scalp EEG taken during active DBS at therapeutic (OnTarget) and non-therapeutic (OffTarget) targets. Using combined emotion self-report and EEG measurements alongside OnTarget stimulation of SCCwm and OffTarget stimulation 1.5 mm away, we trained a *support vector machine* (SVM) capable of confirming precise stimulation. We demonstrate that the learned model coefficients align with *engaged tractography* predicted through volume of tissue activated (VTA) modeling. This compound model will enable implementation, study, and improvement of adaptive SCCwm-DBS, particularly in TRD, more systematic. The classifier is released open source to the community for further validation, refinement, and extension; the dataset is released as a part of a multimodal foundation for antidepressant DBS.

## 1 INTRODUCTION

Deep brain stimulation (DBS) has emerged as a promising, albeit complex, therapeutic option for severe, treatment-resistant psychiatric depression (MDD) in a subset of patients who have not responded to conventional therapies Mayberg et al. (2005); Riva-Posse et al. (2014; 2018). While the clinical efficacy of DBS for MDD has been demonstrated in open-label studies and meta-analyses, a number of large randomized controlled trials have yielded mixed outcomes, highlighting the need for more systematic and precise methods to guide and optimize therapeutic targeting Holtzheimer et al. (2012); Mayberg et al. (2005); Riva-Posse et al. (2014; 2018); Howell et al. (2019).

Systematic study and validation of antidepressant DBS within the SCC requires more objective signatures specific to therapeutic efficacy Smart et al. (2018); Tiruvadi et al. (2022a); Waters et al. (2018); Starr (2018); Stanslaski et al. (2012; 2018). Since an equivocal trial, evidence has emerged that broad DBS of the SCC is insufficient to achieve sustained antidepressant response - rather precise stimulation of SCCwm is needed, likely with individualized tractography. The subcallosal cingulate white matter (SCCwm) has been a primary target for DBS in MDD, based on its role as a critical node within a mood-regulating brain network. However, the mechanism by which stimulation of this region alleviates symptoms is still an active area of investigation, and the precise anatomical and electrophysiological signature of effective stimulation remains unclear. Early investigations have identified a network of brain regions are likely targets for successful antidepressant DBS Tiruvadi et al. (2022a;b); Waters et al. (2018) but data heterogeneity and the high dimensional variances of clinical care make standard analyses insufficient.

In this study, we present a machine learning-based approach to address these challenges by leveraging scalp neural recordings to identify and validate a precise stimulation target. We introduce a regularized support vector machine (SVM) classifier capable of distinguishing precise DBS of the SCCwm ("OnTarget") from nearby stimulation ("OffTarget"), as confirmed by emotional self-responses and VTA analysis. This work advances the field of neuromodulation by providing a

foundational model that can serve as an anchor for future systematic clinical trials and rational engineering of adaptive DBS systems.

## 2 METHODS

### 2.1 PATIENTS AND OUTCOME

Six consecutive patients were implanted between June 1, 2013 and January 1, 2017 as a part of an IRB approved research protocol at Emory University studying the SCCwm-DBS for TRD (ClinicalTrials.gov Identifier NCT01984710) using inclusion and exclusion criteria. Written informed consent was provided by each patient to participate in the study protocol (FDA IDE G130107) and the study was continuously monitored by the Emory University Department of Psychiatry and Behavioral Sciences Data and Safety Monitoring Board. All patients completed the PC+S™ study, continuing until the battery was depleted, and were treatment responders beyond 12 months Stanslaski.

### 2.2 TRACTOGRAPHY AND IMPLANTATION

Pre-operative diffusion tractography was used to individually target DBS implants to a specific intersection of four white matter bundles in the subcallosal cingulate white matter (SCCwm). During implantation, each bilateral DBS lead was placed to ensure an electrode precisely in the target ("OnTarget") for therapy, leaving another adjacent ("OffTarget") as an experimental contrast 1.5 mm. The neural structures activated by each electrode were then computationally modeled using an "engaged tractography" technique, which analyzes the volume of tissue activation in relation to the patient's unique white matter anatomy.

### 2.3 DBS AND EXPERIMENT

Patients were brought in four weeks after implantation, with chronic stimulation inactive throughout, for an experiment day and subsequent therapeutic stimulation initiation. Chronic, therapeutic stimulation was initiated at 3.5 V and 130 Hz, 90  $\mu$ s pulsewidth, monopolar at the OnTarget stimulation site *bilaterally*. Experimental stimulation was performed at both OnTarget and OffTarget targets at 6 mA; otherwise identical parameters as chronic, therapeutic stimulation. Stimulation was delivered for 3 min with 1 min washout immediately before and after, and a 20 min washout was done between Targeting changes.

### 2.4 EMOTION SELF REPORT

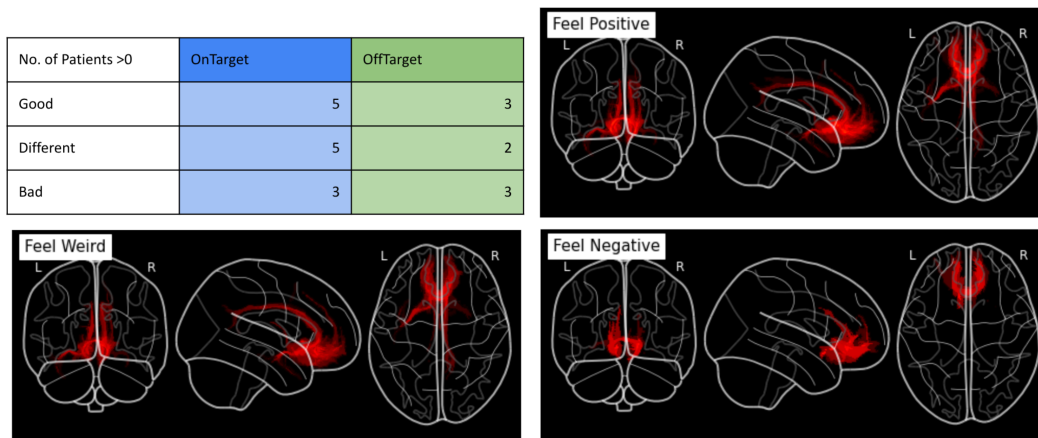
Patients were blinded to stimulation condition (On or Off) and configuration (OnTarget, OffTarget, laterality). Patients were presented with three buttons and told to press the button best corresponding to their emotion and/or sensation at any time. Button presses were summed within each stimulation condition and reported as associated with the corresponding configuration.

### 2.5 NEURAL RECORDINGS

EEG Acquisition Dense-array electroencephalography (dEEG) timeseries were collected with a 256-channel Hydrocel Geodesic Sensor Net (Electrical Geodesics Inc., Eugene, OR) and Netstation data-acquisition software (Electrical Geodesics Inc., Eugene, OR). Channels are sampled at 1 kHz and referenced against Cz. All electrode impedances were maintained below 50 k $\Omega$  and checked every 20 min. Hardware filtering was performed at 100 Hz low-pass and a 0.1 Hz highpass to remove just high-frequency noise and baseline DC offsets. Patients were seated comfortably in a climate-controlled environment with head positioned with an adjustable chin rest. During all recordings patients were told to blink naturally, and relax muscles in shoulders, neck, face.

### 2.6 OSCILLATORY POWER FEATURES

**Time-Frequency and Oscillatory States** All recordings are transformed into the time-frequency domain using STFT and overlapping Welch windows. Parameters were kept constant for the Welch



123 Figure 1: **Self-reported Emotion Changes**. Top Left: Table of responses under OnTarget and Off-  
124 Target stimulation. OnTarget exhibited more overall responses than OffTarget, and these responses  
125 were mostly not 'bad'. Others: The engaged tractography associated with each of the self-reported  
126 emotions evoked.

127  
128 estimate of the PSD, and oscillation frequency windows are fixed at the MC adjusted ranges - con-  
129 sistent across both LFP and EEG. We calculate these features for all LFP+EEG channels (258  
130 total) across all segments (total of approximately 600, depending on stringency of preprocessing).  
131 The brain's instantaneous oscillatory state is measured as a vector  $\vec{\theta}_t \in \mathbb{R}^{256 \times 4}$ .  
132

133 **Oscillatory Responses** Median power was calculated in each oscillatory feature across all pre-  
134 stimulation segments Tiruvadi et al. (2022b) This median power is subtracted from each peri-DBS  
135 segment, yielding a *response vector*. Response vectors are used for classifier training and assess-  
136 ment, and all segments from the EEG patient subcohort are used to build a training curve and deter-  
137 mine the optimal number of segments to use in classifier training.  
138

## 139 2.7 SUPPORT VECTOR MACHINE

140  
141 A support vector machine (SVM) was chosen for its robustness in classifying high-dimensional  
142 brain signals. We implemented a 2-class linear SVM with an  $L_1$  regularizer using Python's  
143 `scikit-learn` library to map baseline-corrected oscillatory responses from EEG channels to  
144 their corresponding stimulation class, either {OnTarget} or {OffTarget}. The classifier was trained  
145 on a balanced set of data segments and tested on subsampled segments from a held-out testing set.  
146 The use of an  $L_1$  regularizer also enabled the identification of a sparse subset of EEG channels for  
147 the classification task.

## 148 2.8 CODE AVAILABILITY

149  
150 Code is openly available at **redacted**. Model coefficients and associated architecture are available  
151 at **redacted**  
152

## 153 3 RESULTS

### 154 3.1 EMOTIONS EVOKED

155  
156 Patient self-reported button presses demonstrate a clearly differential pattern across stimulation tar-  
157 get (Figure 1). OnTarget is predominantly not 'bad' while OffTarget is evenly split. The response  
158 rates are too small to perform robust statistical testing, but speculation from early trends may align  
159 with short-term electrophysiology Sendi et al. (2021). In all cases, patients are placed OnTarget  
160 chronically - n=5/6 patients were long-term responders to treatment at 6 months, all n=6/6 patients  
161 were responders at 12+ months.

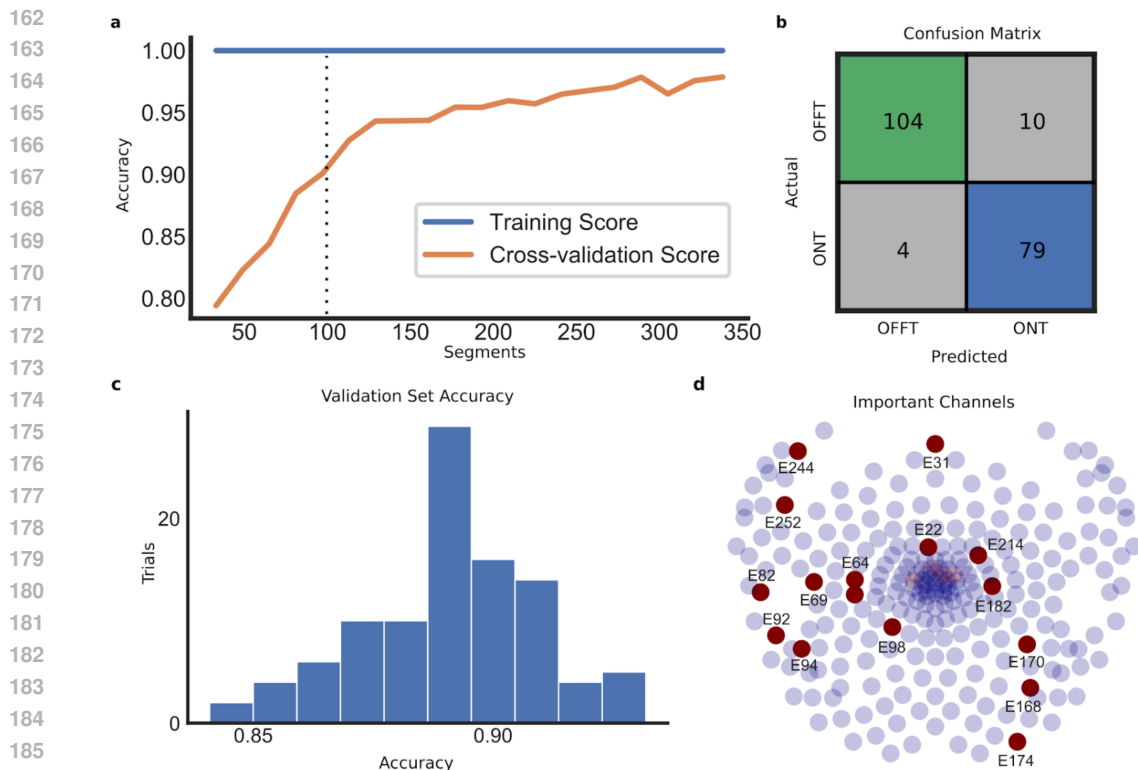


Figure 2: **Classifier Training, Error, and Performance.** a) Training curve demonstrates quick convergence to 90% accuracy with only 30% of segments. b) Errors are predominantly misclassification of OffTarget as OnTarget. c) Bootstrapped validation set across 100 trials demonstrates high accuracy in unseen segments. d)  $L_1$ -regularized SVM coefficient magnitudes across all oscillatory powers align along left temporal and right parietal dEEG channels.

### 3.2 TARGETING CLASSIFIER

**Training** The trained  $L_1$ -regularized SVM achieved a high performance inside the training set, with performance plateauing at 0.95 with 33% of the available segments used to train (Figure 2a). The final SVM is trained on 100 random segments (Figure 2a).

**Testing and Performance** In a single assessment trial consisting of the remaining 250 segments, the classifier achieves 90% accuracy in binary classification (Figure 2b). With a bootstrapped estimate of the classifier accuracy, an average of 0.89 accuracy in binary classification is found over 100 trials (2c).

**Errors and Coefficients** Errors are primarily in misclassification of OffTarget as OnTarget (Figure 2b) and not vice-versa. Overlap in tractography may explain this as OnTarget and OffTarget are likely to hit some shared tracts (Figure 3). The coefficients lie largely along the left temporal and right parietal regions (Figure 2d).

### 3.3 TRACTOGRAPHIC ALIGNMENT

**Useful Channels** To isolate the most informative EEG channels the SVM training procedure is regularized with an  $L_1$  penalty (Figure 2d). The resulting mask demonstrates an asymmetry: left temporal channels and right parietal channels are in the top 10% of largest coefficient  $L_2$  norms.

**Whole-brain Connectomic Masking** We propose a final filtering step to yield a *direct antidepressant circuit* mapped from the direct effects of antidepressant OnTarget SCCwm-DBS (Figure

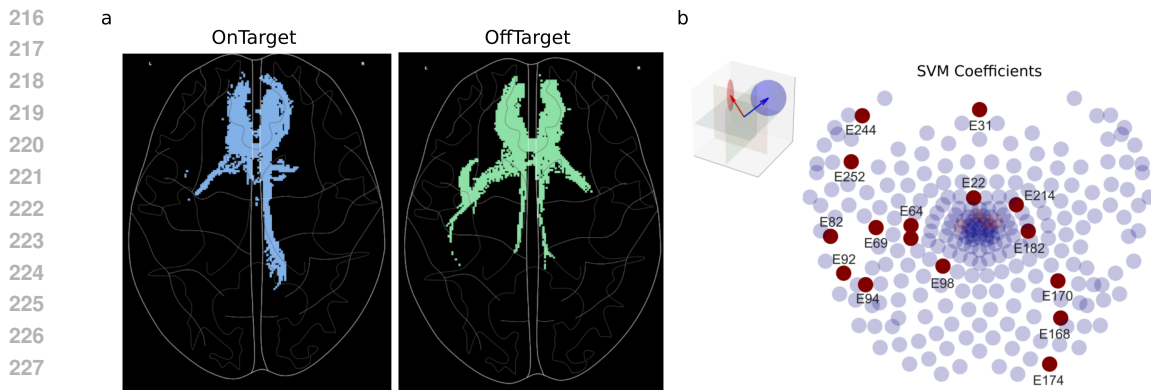


Figure 3: **Alignment of Targeted Tractography and SVM Coefficients.** a) OnTarget and OffTarget Engaged Tractography difference. Demonstrates which voxels are engaged more under OnTarget (blue) and OffTarget (green), respectively. b) Top 10% of classifier coefficients in a max across any oscillatory band calculation. Follow a left temporal and right parietal asymmetric pattern.

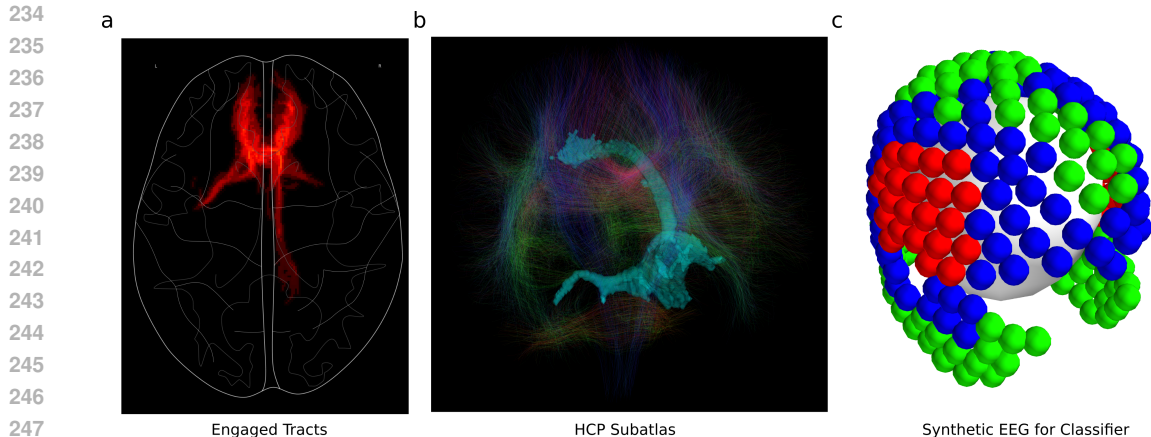


Figure 4: **Pipeline for Generative Connectomics.** a) Engaged tracts under OnTarget stimulation. b) Engaged tractography mask is used to filter the Human Connectome Project (HCP900) structural connectome. c) Filtered tracts can be used to generative synthetic EEG signals for comparison with empirical oscillatory changes.

4). To do this, we coregistered our engaged tractography map, with binary threshold, with an openly available HCP-based dMRI connectome Li et al. (2020) to identify the key fibers involved (Figure 4b). Masks for OnTarget and OffTarget are used to filter out the streamlines associated with each of the emotions evoked in Figure 1 Table. The resulting synthetic EEG can be used to fine tune the SVM based on patient-specific dMRI (Figure 4c).

## 4 DISCUSSION

Classifiers that can use neural recordings to confirm adequate DBS implantation and stimulation are needed for more systematic implementation and study of therapy, especially in psychiatric disorders like depression. In this study, we reanalyzed a previously reported set of data Tiruvadi et al. (2022b) using ML to build a classifier capable of determining precise SCCwm-DBS, and then linking the classifier coefficients to tractography and self-reported emotion.

Noninvasive recordings provide evidence that stimulation just 1.5 mm away from the target can evoke a distinctly different neural state, measured in both temporal evoked potential Tiruvadi et al. (2022a) and spectral responses Tiruvadi et al. (2022b). Our classifier provides an alternative look at

270 that evidence, with a more direct link between engaged tractography and scalp response (Figure 3).  
271 By interpreting electrophysiology through the lens of anatomy, we use the tractography from surgi-  
272 cal planning as a scaffold to analyze brain-wide oscillatory responses to SCCwm-DBS. Calculation  
273 of engaged tractography confirms that OnTarget stimulation engages asymmetric white matter tracts,  
274 specifically the right cingulum bundle (right-CB), which emerges as a major differentiator consist-  
275 ent with a growing body of literature Howell et al. (2019); Riva-Posse et al. (2018); Tsolaki et al.  
276 (2021). In contrast, OffTarget stimulation engages more symmetric tracts and the left uncinate fas-  
277 ciculus (left-UF). The observed  $\alpha$  response and other oscillatory dynamics align spatially with these  
278 engaged tracts, suggesting that SCCwm-DBS evokes dynamics reflecting the structural and synaptic  
279 processes of the underlying networks, which is consistent with a biphasic mechanism of action and  
280 has implications for linking brain structure to changes in mood.

281 Leveraging these findings, we developed a supervised learning model as a potential target engage-  
282 ment classifier to distinguish neural signals caused by therapeutic OnTarget versus nearby OffTarget  
283 stimulation. A linear classifier achieved approximately 90% testing accuracy in this task (Figure 2)  
284 and identified right-parietal and left-temporal channels as the most informative, corroborating the  
285 tract differences found in our DTI analysis (Figure 3).

286 This study has several limitations. First, the small sample size of six patients is limiting to gener-  
287 alization. However, the full population of patients that receive SCCwm-DBS is small, and this is a  
288 study of a sizable portion of that population. Second, The low number of self-report emotion button  
289 clicks limits our ability to make strong statements about the exact nature of OnTarget and OffTarget  
290 effects on emotion. Third, the SVM performance is reported in-sample due to limited size. Addi-  
291 tionally, while training and testing never overall in the temporal segment used, they are still taken  
292 from the same task and intrinsic autocorrelations could bias results. The alignment of coefficients to  
293 tractography is taken as a mitigation of this, but the limitation must be addressed moving forward.  
294 Finally, it remains unclear if engagement of OnTarget at 6 mA is desired as this is above therapeutic  
295 values. Attempting to evoke the same state as suprathreshold stimulation may not be therapeutic,  
296 and a more direct experiment at therapeutic parameters will be done.

## 297 5 CONCLUSION

298 We trained an ML classifier on previously reported scalp EEG signatures of precise SCCwm-DBS  
299 to build a model capable of identifying OnTarget SCCwm-DBS from scalp electrodes. While fur-  
300 ther testing is needed, the classifier’s performance and its alignment with anatomical tractography  
301 provide preliminary confidence in this approach for developing a physiologic readout for adaptive  
302 DBS therapy in MDD and/or SCCwm-DBS. Future work will focus on optimizing classification  
303 while minimizing the number of EEG electrodes, and more explicitly integrating neural dynamics  
304 into the classification task Tiruvadi et al. (2022a), potentially as ANNs or latent state space models.  
305 The classifier will be released open source to the community for further validation, refinement, and  
306 extension to enable more reliably implantation and engineer adaptive antidepressant DBS systems.  
307  
308

## 309 REFERENCES

- 310 Paul E Holtzheimer, Mary E Kelley, Robert E Gross, Megan M Filkowski, Steven J Garlow, Andrea  
311 Barrocas, Dylan Wint, Margaret C Craighead, Julie Kozarsky, Ronald Chismar, et al. Subcallosal  
312 cingulate deep brain stimulation for treatment-resistant unipolar and bipolar depression. *Archives*  
313 *of General Psychiatry*, 69(2):150–158, 2012.
- 314 Bryan Howell, Ki Sueng Choi, Kabilar Gunalan, Justin Rajendra, Helen S Mayberg, and Cameron C  
315 McIntyre. Quantifying the axonal pathways directly stimulated in therapeutic subcallosal cingu-  
316 late deep brain stimulation. *Human brain mapping*, 40(3):889–903, 2019.
- 317 Ningfei Li, Juan Carlos Baldermann, Astrid Kibleur, Svenja Treu, Harith Akram, Gavin JB Elias,  
318 Alexandre Boutet, Andres M Lozano, Bassam Al-Fatly, Bryan Strange, et al. A unified connec-  
319 tomic target for deep brain stimulation in obsessive-compulsive disorder. *Nature communications*,  
320 11(1):3364, 2020.

- 324 Helen S Mayberg, Andres M Lozano, Valerie Voon, Heather E McNeely, David Seminowicz,  
325 Clement Hamani, Jason M Schwalb, and Sidney H Kennedy. Deep brain stimulation for  
326 treatment-resistant depression. *Neuron*, 45(5):651–660, 2005.
- 327  
328 Patricio Riva-Posse, Ki Sueng Choi, Paul E Holtzheimer, Cameron C McIntyre, Robert E Gross,  
329 Ashutosh Chaturvedi, Andrea L Crowell, Steven J Garlow, Justin K Rajendra, and Helen S  
330 Mayberg. Defining critical white matter pathways mediating successful subcallosal cingulate  
331 deep brain stimulation for treatment-resistant depression. *Biological psychiatry*, 76(12):963–969,  
332 2014.
- 333 Patricio Riva-Posse, KS Choi, Paul E Holtzheimer, Andrea L Crowell, Steven J Garlow, Justin K Ra-  
334 jendra, Cameron C McIntyre, Robert E Gross, and Helen S Mayberg. A connectomic approach for  
335 subcallosal cingulate deep brain stimulation surgery: prospective targeting in treatment-resistant  
336 depression. *Molecular Psychiatry*, 23(4):843–849, 2018.
- 337 Mohammad SE Sendi, Allison C Waters, Vineet Tiruvadi, Patricio Riva-Posse, Andrea Crowell,  
338 Faical Isbaine, John T Gale, Ki Sueng Choi, Robert E Gross, Helen S Mayberg, et al. Intraoper-  
339 ative neural signals predict rapid antidepressant effects of deep brain stimulation. *Translational*  
340 *psychiatry*, 11(1):1–7, 2021.
- 341  
342 Otis Smart, Ki S Choi, Patricio Riva-Posse, Vineet Tiruvadi, Justin Rajendra, Allison C Waters,  
343 Andrea L Crowell, Johnathan Edwards, Robert E Gross, and Helen S Mayberg. Initial unilateral  
344 exposure to deep brain stimulation in treatment-resistant depression patients alters spectral power  
345 in the subcallosal cingulate. *Frontiers in Computational Neuroscience*, 12:43, 2018.
- 346 Scott Stanslaski. email.
- 347  
348 Scott Stanslaski, Pedram Afshar, Peng Cong, Jon Giftakis, Paul Stypulkowski, Dave Carlson, Dave  
349 Linde, Dave Ullestad, Al-Thaddeus Avestruz, and Timothy Denison. Design and validation of  
350 a fully implantable, chronic, closed-loop neuromodulation device with concurrent sensing and  
351 stimulation. *IEEE Transactions on Neural Systems and Rehabilitation Engineering*, 20(4):410–  
352 421, 2012.
- 353 Scott Stanslaski, Jeffrey Herron, Tom Chouinard, Duane Bourget, Ben Isaacson, Vaclav Kremen,  
354 Enrico Opri, William Drew, Benjamin H Brinkmann, Aysegul Gunduz, et al. A chronically  
355 implantable neural coprocessor for investigating the treatment of neurological disorders. *IEEE*  
356 *transactions on biomedical circuits and systems*, 12(6):1230–1245, 2018.
- 357 Philip A Starr. Totally implantable bidirectional neural prostheses: a flexible platform for innovation  
358 in neuromodulation. *Frontiers in Neuroscience*, 12:619, 2018.
- 359  
360 Vineet Tiruvadi, Ki Sueng Choi, Robert E Gross, Robert Butera, Viktor Jirsa, and Helen S May-  
361 berg. Dynamic oscillations evoked by subcallosal cingulate deep brain stimulation. *Frontiers in*  
362 *neuroscience*, pp. 85, 2022a.
- 363 Vineet R Tiruvadi, Ki Sueng Choi, Allison Waters, Liangyu Tao, Rohit Konda, Nasir Ibrahim, Otis  
364 Smart, Andrea Crowell, Patricio Riva-Posse, Robert E Gross, et al. Network action of subcallosal  
365 cingulate white matter deep brain stimulation. *medRxiv*, pp. 2022–07, 2022b.
- 366  
367 Evangelia Tsolaki, Sameer A Sheth, and Nader Pouratian. Variability of white matter anatomy in  
368 the subcallosal cingulate area. *Human Brain Mapping*, 2021.
- 369 Allison C Waters, Ashan Veerakumar, Ki Sueng Choi, Bryan Howell, Vineet Tiruvadi, Kelly R Bi-  
370 janki, Andrea Crowell, Patricio Riva-Posse, and Helen S Mayberg. Test–retest reliability of a  
371 stimulation-locked evoked response to deep brain stimulation in subcallosal cingulate for treat-  
372 ment resistant depression. *Human Brain Mapping*, 39(12):4844–4856, 2018.

## 374 A APPENDIX

375  
376  
377